



Article Type : Research Article  
Received : December 4, 2024  
Revised : March 5, 2025  
Accepted : March 7, 2025  
DOI : [10.17798/bitlisfen.1596470](https://doi.org/10.17798/bitlisfen.1596470)

Year : 2025  
Volume : 14  
Issue : 1  
Pages : 435-463



## URBAN HEAT ISLAND EFFECT OF LARGE-SCALE RESIDENTIAL AREAS: A SPATIOTEMPORAL ANALYSIS OF ETİMESGUT DISTRICT IN ANKARA

Büşra Hilal KUTLU AYDIN<sup>1\*</sup> , Burcu Halide ÖZÜDURU<sup>1</sup> 

<sup>1</sup> Gazi University, Department of City and Regional Planning, Ankara, Türkiye

\* Corresponding Author: [hilalkuthu@gazi.edu.tr](mailto:hilalkuthu@gazi.edu.tr)

### ABSTRACT

Urban heat islands (UHI) disrupt the environmental balance in urban areas. The rate and impact of this formation are intensified by the increase in impervious surfaces, along with urban sprawl and land use changes. This increase reduces natural water absorption, causing heat retention and airflow restriction. Changes in land cover alter surface albedo, affecting energy interactions between the atmosphere and the surface, leading to local climate change. Remote detection methods are important tools for data gathering and assessing UHIs. This study uses a spatiotemporal analysis to examine the relationship between urban development and UHI change between 2005 and 2021, focusing on the Etimesgut district, located on the western development axis of Ankara, where land use changed from agricultural and public land to large-scale residential areas in the last three decades, in particular along with the development of mass housing by Housing Development Agency. Therefore, the district was under pressure for urban growth and mainly developed by transferring public property to private property. The analysis explains how urban sprawl increases land surface temperature (LST), contributing to the formation of UHIs. This study shows that in the Etimesgut district, where the built-up area has increased significantly between 2005 and 2021, from 9,040 ha to 12,934 ha, showing a 43.08% increase, there has been an increase in the LST by about four °C, rising from 43.33°C to 47.02°C in July. Satellite imagery-based findings indicate that the replacement of agricultural land by built-up areas accelerates the rise in temperatures in the region by weakening natural cooling mechanisms. This study intends to inform urban policy and policy development and offers an evidence-based approach using the Etimesgut district in Ankara as a case study. Urban development policies should cover climate-prone strategies and thermal governance to mitigate the UHI effects when barren or agricultural land is replaced with impervious surfaces of large-scale residential areas.

**Keywords:** Climate change, Urban Heat Island (UHI), Land Surface Temperature (LST), Urban growth, Land use change.

## 1 INTRODUCTION

Sustainable development is defined as "development that meets the needs of the present without compromising the ability of future generations to meet their own needs" (WCED, 1987), achieved through a balance among environmental, social, and economic factors. Its widespread adoption began with the Brundtland Report (1987). It was reinforced by subsequent initiatives such as the 1992 Earth Summit, Local Agenda 21 (LA21) publications, the European Commission's Green Papers, and the OECD's environmental policy reports for cities. These efforts aimed to address energy consumption, CO<sub>2</sub> emissions, and waste management to mitigate the impacts of rising temperatures, sea-level rise, and extreme weather events [1]. The relationship between sustainable development and urban heat islands (UHIs) has emerged as a critical study area. UHIs result from urbanization-induced factors such as reduced vegetation, increased impervious surfaces, and anthropogenic heat emissions, which raise urban temperatures, degrade air quality, and pose significant public health risks. Reducing UHI effects through energy-efficient urban design, green infrastructure expansion, and climate adaptation strategies aligns directly with sustainable development goals. Thermal governance thus offers a strategic framework to enhance urban resilience, improve living conditions, and contribute to global efforts against climate change [2].

Urban areas are key to globalization and development models and show the evident transition to new land use types [3]. Research on UHIs has gained particular attention due to the impact of this transition on energy consumption in buildings, human comfort, air pollution, and urban ecology [4]. UHI forms when an urban area is warmer than the surrounding rural areas, with temperature differences observable on the surface or in the air, particularly near the ground. This phenomenon is influenced by surface energy and radiation balance accompanying urban development, as well as by natural factors, urban form and function, and time, which shows daily and seasonal variability [5]. The increase in air temperature leads to a decline in the quality of urban livability, thus giving rise to urban heat stress [4].

The UHI effect can impact local weather and climate by altering wind patterns and precipitation rates [6]. Impervious surfaces in cities, including building roofs, parking lots, roads, transportation infrastructure, tall buildings, and areas without vegetation (e.g., sandy or barren regions), primarily contribute to the UHI effect due to air trapping and airflow reduction [7]. The thermal balance in the built environment is defined as the sum of heat gains, heat storage, and heat losses. Since urban areas experience higher heat gains and lower heat losses

than surrounding rural or urban environments, the thermal balance in these areas is higher, leading to elevated ambient temperatures compared to rural regions. [8].

Residential areas typically consist of impervious surfaces, which act as barriers to water infiltration into the ground. The increase in impervious surface areas is the primary driver of hydrological and environmental changes linked to urban growth [9]. Changes in land use and land cover alter the surface albedo (reflectance or reflectivity), which enhances energy interactions between the atmosphere and the surface, leading to local climate impacts. Land use changes lead to alterations in LST [10]. Due to variations in land use and land cover (LULC) changes, the albedo, thermal conductivity, capacity, and retention of surfaces are affected [11].

Each city's LULC varies by its unique urban structure, the primary construction materials of the built environment, population density, shape, size, arrangement of buildings, planning strategies, and growth dynamics [12]. The increase in global warming is linked to LULC changes, with temperature fluctuations in urban centers being notably higher than in surrounding areas [13].

Population growth in cities and economic and functional expansion also alters urban morphology. This transformation necessitates the addition of physical structures such as housing, offices, industrial zones, commercial spaces, and transportation infrastructure to support urban activities [14]. Increasing population density, the expansion of residential areas, the rise in buildings and impervious surfaces, the type of construction materials used, greater vehicular traffic, excessive energy consumption, air pollution, and poor air circulation all contribute to changes in urban microclimates [15], [16]. To accommodate urban growth, cities expand beyond their urban boundaries, placing pressure on surrounding natural resources and replacing wetlands, vegetation, and agricultural land [17]. Economic development in cities often leads to new industrial zones, public infrastructure, open spaces, and residential developments. Urban sprawl, with the conversion of vegetative and barren lands near cities into urban areas, exacerbates the UHI effect [18] and causes changes in ecology, biodiversity, landscapes, and natural habitats [19]. The biophysical characteristics of urban spaces are key determinants of the local climate.

Remote sensing methods have proven to be valuable in understanding the LULC change. Earth observation data are widely used to assess the effects of UHI spatial distribution, urban vulnerabilities, and health-related risks [20]. Surface UHI is typically measured using

LST derived from thermal remote sensing, providing an opportunity to characterize UHI formation across various temporal scales (daily, seasonal, and annual) [4].

Various land cover indices have been developed to investigate the relationships between land cover changes and land surface temperature (LST). One such index is the Normalized Difference Vegetation Index (NDVI), which is utilized to assess vegetation density on a global scale, monitor drought events, track and predict agricultural productivity, identify fire-prone areas, and map desertification processes [21]. The correlation between NDVI and LST indicates that changes in vegetation cover can significantly influence surface temperatures. In particular, areas with dense vegetation are often associated with lower surface temperatures, highlighting the critical cooling effect of vegetation.

This study uses spatiotemporal analysis to examine the relationship between LULC change and the UHI. It focuses on the Etimesgut district in Ankara, a new development area, to identify how urban sprawl impacts local climate dynamics and contributes to the intensification of the UHI effect. This study investigates how land use changes from agriculture to large-scale residential areas between 2005 and 2021, influence the change in UHIs by increasing LST. The findings are evaluated in order to define how urban sprawl has an impact on a city, Ankara. Following the introduction, the second section explains the data and methods used. The third section presents the study's main findings, while the final section evaluates the results concerning urban policy and strategies.

## **2 STUDY AREA, DATA AND METHODOLOGY**

### **2.1 Study Area**

Ankara is the capital city of Türkiye, and it is experiencing a rapid population increase. The population, recorded at 4.466.756 in 2007, increased to 5,747,325 by 2021, representing a growth rate of 28,67% [22]. The growth of the city as a result of this increase has been influenced by various factors. These factors include the site selection of public institutions in the city center following the Jansen Plan, the first plan implemented, and the industrial and residential development zones designated after the Yücel-Uybadin Plan in 1957, the second plan implemented. Particularly, the increasing residential areas after the 1950s and the rise in informal housing (squatters) from the 1960s onwards contributed to Ankara's significant growth [41]. In the 1970s, particularly in the 1990s, the city expanded along its West, on the Istanbul and Eskisehir highways, with many public institutions and university campuses [23].

With the 1990 Master Plan, Ankara's previously monocentric and compact urban form transformed into a polycentric structure, where the population shifted towards newly developed residential areas and urban development occurred along various axes. The 1990 Master Plan developed the first strategies and planning decisions to overcome the city's geographic constraints, shaping Batıkent, Sincan, and Cayyolu as large-scale residential areas located on the periphery, outside the central core [24]. In the 2023 Ankara Master Development Plan, residential development trends continue to expand along this corridor, reinforcing the decentralization policies of the 1990 Master Plan. The Etimesgut district is also designated as a large-scale residential area shaped by these plans. As a result of the LULC analysis conducted using Landsat satellite images, the built-up area in Ankara has increased from approximately 126,569 hectares in 2005 to approximately 162,586 hectares in 2021, reflecting a 28.46% increase.

In this context, the Etimesgut district was initially planned as part of the western development corridor, followed by the southwestern development corridor, emerging sequentially after the Batıkent-Sincan and Çayyolu satellite towns as a new growth area. The concentration of urban work zones in the district and the planning of large-scale residential areas after the 1980s have highlighted the residential regions. These planned developments were supported by social amenities and the strategic location of significant public buildings during this period. With the suburbanization process accelerating urban growth around the city, Etimesgut has undergone a transformation in housing typology, shifting from mass housing to luxury residential developments, making the district a significant hub in terms of housing, public structures, and infrastructure along with the urban development process accelerating urban growth around the district. The concentration of business zones and large-scale residential areas in the district after the 1980s has highlighted the significant change from agricultural to built-up land. Urban amenities supported these planned developments.

Neighborhoods within the Etimesgut district, such as Eryaman, Elvankent, Yaprıcık, and Bağlıca, have also become important residential areas following investments and urban growth after the 2000s. In particular, the large-scale residential developments in the district were significantly influenced by the mass housing projects initiated by the Housing Development Agency, which facilitated the transformation of land use from agricultural and public land to extensive residential areas over the last three decades. As a result, urban growth in Etimesgut was primarily driven by the transfer of public property to private property, placing the district under significant development pressure. The Etimesgut district was selected as the

study area due to the rapid population increase in Ankara following the declaration of the Republic and its designation as the capital, which accelerated the urbanization process and increased urban density. As urban density grew, new development corridors were planned, and growth along these corridors exceeded expectations. Therefore, the Etimesgut district is a key area for examining the impacts and consequences of urban development on the formation of UHIs. Figure 1 shows the district's location in Ankara and the location of neighborhoods in Etimesgut. This area was selected as the study site due to its rapid population increase and expansion, accelerating urbanization, and increasing urban density, contributing to urban sprawl. This study highlights the temperature source for the UHI effect, LULC, and NDVI parameters, focusing on changes between 2005 and 2021. A temperature change profile has been created.

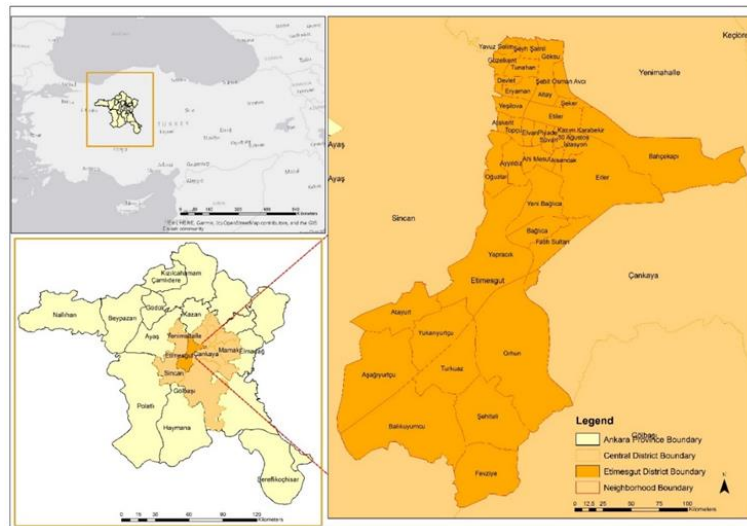


***Figure 1. Study Area: Etimesgut District Boundary and its Neighborhoods.***

## 2.2 Data Sources

Landsat satellite images obtained from USGS (United States Geological Survey) for 2005 and 2021, including LST, land use, vegetation cover (NDVI), and data from Open Street Map (road network and building footprints), high-resolution Google Earth imagery digitization, and field survey data are utilized in this study. There are seven thermal band datasets. Among these, bands 1 to 5 and 7 have a spatial resolution of 30 meters, while the thermal band 6 has a resolution of either 120 meters (TM) or 60 meters (ETM+), depending on the sensor used.

2005 measurements were retrieved using the bands from Landsat 4-5 TM satellite images for each month of the year as follows:

- LST – (bands 3, 4, 6)
- NDVI – (bands 4, 3)

2021 measurements were retrieved using the bands from Landsat 8 TM satellite images for each month of the year as follows:

- LST – (bands 4, 5, 10)
- NDVI – (bands 4, 5)

July data were used following atmospheric and geometric corrections. Table 1 presents the dataset information for the satellite images for 2005 and 2021. According to Table 1, the cloud cover ratio was determined to be 0.02 for 2005 and 0.00 for 2021.

*Table 1. Satellite image dates.*

Year	Month	Day	Time	Sensor	Cloud Cover	Path	Row
2005	July	03.07.2005	08:14	Landsat 4-5 TM	0.02	177	32/33
2021	July	31.07.2021	08:27	Landsat 8 TIRS/ORS	0.00	177	32/33

Ground temperature data from meteorological stations provided by the Turkish State Meteorological Service are used to analyze the accuracy of the LST distribution obtained from satellite data. For 2005 and 2021 satellite data, only seven stations were operated by the Turkish State Meteorological Service in Ankara, and two were in Etimesgut (Table 2).

*Table 2. Meteorological Station Locations in Ankara.*

Station Number	Station Name	District	Latitude (Decimal)	Longitude (Decimal)	Elevation (m)
17127	Airport/Area	District	40.0788	32.5657	838
17128	Ankara Murtet Airport	Kazan	40.1240	32.9992	959
17129	Ankara Esenboga Airport	Cubuk	39.9558	32.6854	806
18250	Etimesgut Airport	Etimesgut	39.9725	32.8639	887
17131	Kecioren/9 (Ankara) Region	Kecioren	39.9343	32.7387	820
17134	Ankara Guvercinlik Airport	Etimesgut	39.8032	32.8434	1115
17137	Golbasi/Ufuk Danishment	Golbasi	39.7985	32.9716	1807

### 2.3 Method

The study method covers three stages. Following retrieving the indices through imagery acquisition, we perform some computations to prepare the data for analysis. NDVI, LST, LULC, Road Network and Built-up Areas, Meteorological, and Population Data have formed the base for analysis. Next, all indices are prepared using various computations (Figure 2). Following these computations, we analyzed the changes in 2005 and 2021. In this section, these stages are discussed in detail.



Figure 2. Flow Chart of Data Retrieval, Computation and Spatio-temporal Analysis Stages.



### 2.3.1 Data Retrieval and Computations

#### Normalized Difference Vegetation Index (NDVI)

Remote sensing technology can monitor vegetation cover. NDVI data is one of the most widely used tools for tracking vegetation. Using the near-infrared (NIR) and red (RED) wavelength bands of satellite imagery, NDVI assesses vegetation greenness, density, and changes in density. When vegetation is dense, reflectance in the red region decreases while reflectance in the near-infrared region increases. This variation is captured by NDVI data analysis [25], [40].

The NDVI value is calculated using the formula  $(\text{NIR} - \text{RED}) / (\text{NIR} + \text{RED})$ .

For Landsat 4 and 5, NDVI is calculated using two bands: Band 3 (RED) and Band 4 (NIR), while for Landsat 8, it is calculated using Band 4 (RED) and Band 5 (NIR).

NDVI ranges between -1 and +1, and areas covered with green vegetation always have a positive NDVI. Water bodies exhibit low reflectance in both spectral channels, resulting in a negative NDVI. The near-infrared (NIR) channel reflects more than the visible (RED) channel for soil. The soil's moisture content and the rainfall that impacts the vegetation in the study area also influence NDVI [38].

#### Land Surface Temperature (LST)

This study uses the classical method, which consists of six steps, for calculating LST. With advancements in remote sensing, LST obtained from satellites (such as Landsat, MODIS, and ASTER) is widely used to evaluate UHIs and analyze the effects of urban warming [26]. Satellite LST data vary depending on the period, resolution, accuracy, and availability. Using formulas from the USGS Landsat 8 handbook, the six-step process is followed to calculate LST from thermal bands (e.g., Landsat or MODIS satellite data). These stages are as follows: Conversion of Pixel Values (DN) to Spectral Radiance Values, Conversion of Spectral Radiance Values to Brightness Temperature Values, Determination of the NDVI, Determination of the Proportion of Vegetation (Pv), Determination of Emissivity (LSE) Values, Determination of LST Values [25].

#### Land Use-Land Cover (LULC)

LULC changes are closely associated with shifts in climatic conditions, which can be detected along with vegetation cover and soil moisture content [20], [27]. In urban areas, the change in LULC is directly related to urban growth and development [28]. Since the 1960s,

multispectral satellite imagery, such as WorldView2 and Landsat, has been a crucial data source for monitoring LULC changes [29]. The images were classified using the *Maximum Likelihood classification*, which helped obtain a LULC classification. The classification helped to categorize land cover into settlement areas, forest areas, vegetation, barren land, and water bodies.

### Population Projection Calculation

To assess the impact of urban population density on temperature, population data for the central districts of the study area for the years 2007 and 2021 were obtained from the Turkish Statistical Institute [22]. The population of Etimesgut was 272,977 in 2007 and 606,472 in 2021. Due to the transition to address-based population registration in 2007, detailed data for the year 2005 was not available. Therefore, the population was projected for 2005, using 2007 data.

The *limited exponential growth method* was used for the population projection. This method assumes that population growth has an upper limit. Initially, the growth rates for each district, the corresponding populations, and the arithmetic average of the selected period (2007, 2013, 2021) growth rates are calculated [32]. The population growth rate ( $k$ ) is calculated using Equation (1). The population in 2005 was 3,881,962 for Ankara and 272,977 for the Etimesgut District.

$$k = \begin{cases} k \leq 1 & \text{if } k = 1 \\ 1 < k < 3 & \text{if } k = \bar{k} \\ k \geq 3 & \text{if } k = 3 \end{cases} \rightarrow k = \left( \sqrt[t_s - t_i]{\frac{N_s}{N_i}} - 1 \right) \times 100 \quad (1)$$

where;

$t_s$ : Population based on the most recent census year,

$t_i$ : Population based on the initial census year,

$N_s$ : Population counted in the most recent census year,

$N_i$ : Population counted in the initial census year.

The projected population is computed after calculating  $k$ , as shown in Equation (2).

$$N_p = N_s \times \left( 1 + \frac{k}{100} \right)^{\text{of years between } t_s \text{ and } t_i} \quad (2)$$

where;

$N_p$ : Projected Population,

$N_s$ : Population counted in the most recent census.

### 2.3.2 Spatio-temporal Analysis

Following the data retrieval and computations, we analyzed the respective changes between 2005 and 2021. Thematic mapping has been useful for following the spatial change between these years. For both years, a cross-sectional display has been in effect. The data, corresponding to July for both years, highlight the differences reflected in the indices. The rise in temperatures is not solely dependent on the amount of vegetation but is also associated with climate change and other environmental factors [33].

## 3 RESULTS AND DISCUSSION

The findings reveal a significant increase in LST in the Etimesgut district between 2005 and 2021. This rise in LST is a clear indicator of the UHI effect.

NDVI: Using the bands from Landsat 4-5 and Landsat 8 satellite images for each month in 2005 and 2021 shows NDVI changes (Figure 3).

As illustrated in Figure 3 (a), the NDVI in 2005 varied between -0.90 and 0.73, while in Figure 3 (b) in 2021, the NDVI varied between -0.57 and 0.86. Positive NDVI indicates a high density of healthy vegetation. The highest NDVI in 2021 was 0.86, compared to 0.73 in 2005, with a %17.8 increase. When the NDVI value falls between 0 and -1, it indicates areas of bare soil, water bodies, or regions without vegetation. In 2005, the lowest NDVI value was -0.90; in 2021, this value increased to -0.57, suggesting a reduction in bare soil areas over the years.

This increase is valid for several neighborhoods; for example, in Eryaman, Alsancak, Ahi Mesut, and Elvankent, urban development created an overall increase in NDVI. Particularly for example, in Eryaman neighborhood (as shown in Figure 3(a) and 3(b)), the NDVI values varied between -0.006 and 0.51 in 2005 and between 0.049 and 0.66 in 2021; in the Alsancak neighborhood, the values ranged from -0.01 to 0.37 in 2005 and from 0.02 to 0.58 in 2021; and the Ahi Mesut neighborhood, the values varied between 0.05 and 0.42 in 2005 and between -0.23 and 0.69 in 2021; the Elvankent neighborhood, the values ranged from 0.05 to 0.42 in 2005 and from 0.02 to 0.67 in 2021. These neighborhoods experienced rapid development due to the development of large-scale residential areas. Along with this intensification, the increase in vegetation density in non-urbanized areas, the conversion of agricultural activities into active green spaces, and the implementation of green space designs within urbanized zones have

collectively contributed to a general increase in NDVI values. The relationship between NDVI and LST indicates that changes in vegetation can influence LST.

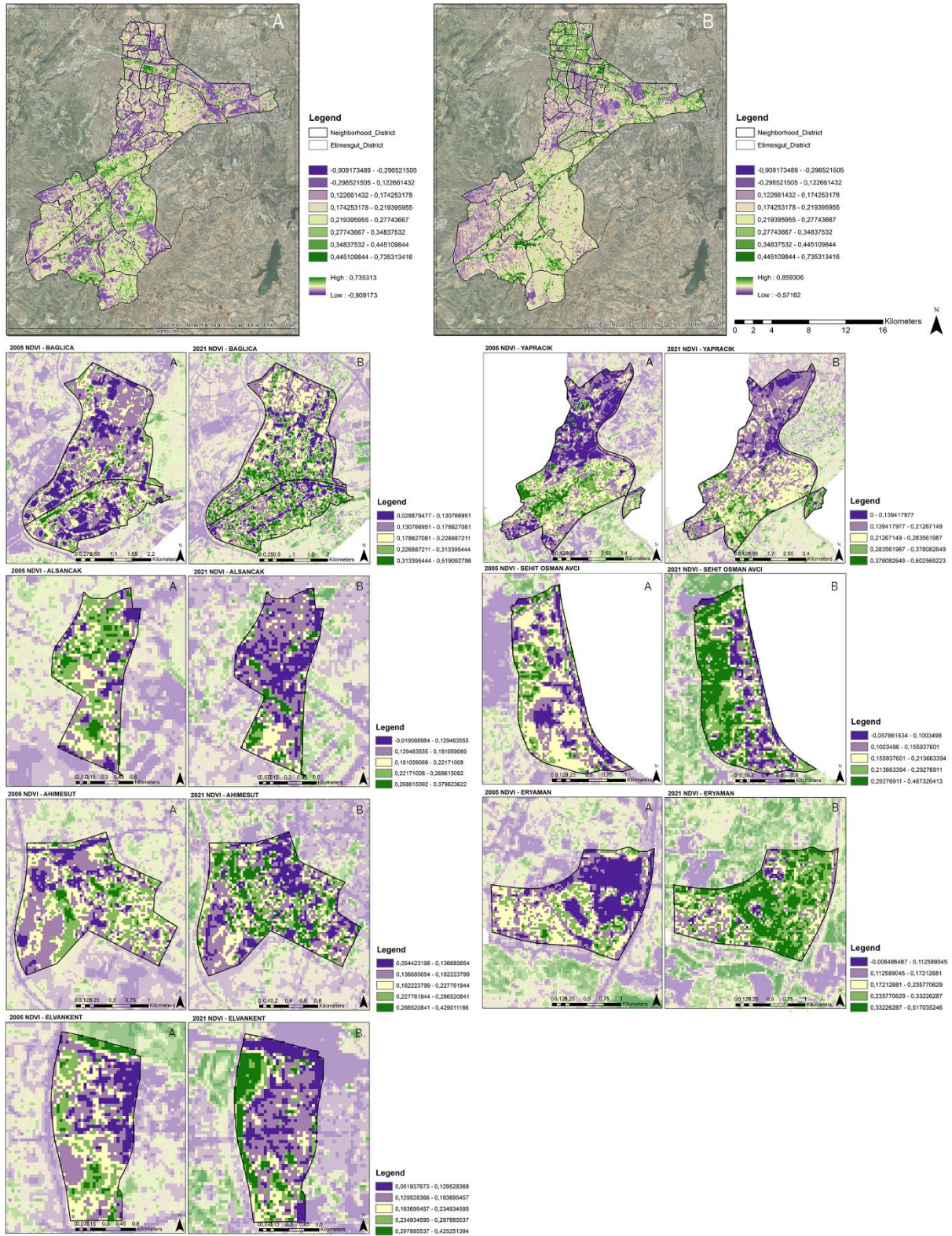


**Figure 3. (a) NDVI of Etimesgut District (2005), (b) NDVI of Etimesgut District (2021).**

The analysis shows that in 2005, the NDVI values for the Bağlıca, Yapracık, and Şehit Osman Avcı neighborhoods of Etimesgut were high, reflecting their rural character with agricultural land and large green spaces. In the Bağlıca neighborhood, the NDVI values varied between 0.02 and 0.51 in 2005 and between 0.02 and 0.67 in 2021; in the Yapracık neighborhood, the values ranged from 0.00 to 0.60 in 2005 and from -0.13 to 0.77 in 2021; and Şehit Osman Avcı neighborhood, the values varied between -0.05 and 0.48 in 2005 and between -0.30 and 0.67 in 2021. However, by 2021, urban development has significantly increased, particularly in Bağlıca and Yapracık. These areas experienced a sharp decline in NDVI values due to large-scale residential areas and social amenities, reducing green spaces. For example, Yapracık, in particular, was rapidly developed with large-scale residential projects of the Housing Development Agency, and the 2021 map shows low NDVI values, indicating the severe built-up area increase in the area.

According to the 2018 Urban Atlas Street Tree Layer data by Land Copernicus (Figure 4), the total area of street trees in Etimesgut is 11.01 km<sup>2</sup>, which constitutes approximately 3.76% of the total surface area of 292.558528 km<sup>2</sup>. This data indicates that the density of trees in the region is limited, and treeless grass areas predominantly characterize the landscape. The limited presence of broad-leaved trees and the predominance of treeless grasslands in Etimesgut are critical factors to consider in land surface temperature (LST) assessments, as the structure of the vegetation directly influences the distribution and intensity of surface temperatures.

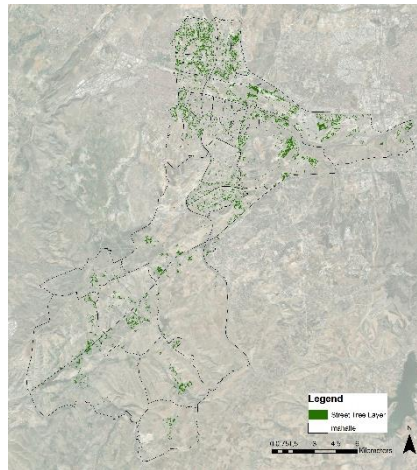


**Figure 4. 2018 Urban Atlas Street Tree Layer of Etimesgut.**

LST: LST thematic maps for the Etimesgut district were created using the thermal bands from Landsat 4-5 and 8 satellite images for each month in 2005 and 2021 (Figure 5a-5b).

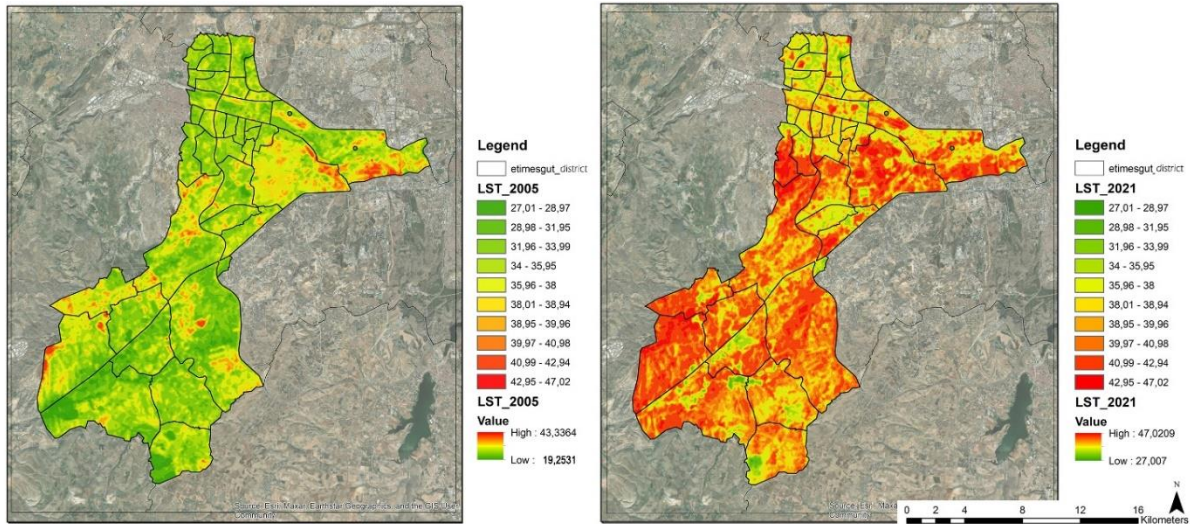


**Figure 5. (a) LST of Etimesgut District (2005), (b) LST of Etimesgut District (2021).**

The highest recorded temperature in July 2005 was 43.33°C; in July 2021, it reached 47.02°C (Figure 5a). This indicates that the hottest days in July 2021 were approximately 4°C warmer than in 2005. This temperature increase is a clear indicator of global warming and climate change, influenced by various factors such as extreme heat events, urbanization, deforestation, and rising greenhouse gas emissions.

In July 2005, the lowest recorded temperature was 19,25°C; in July 2021, it significantly increased to 27°C (Figure 5b). This change indicates a reduction in the difference between daytime and nighttime temperatures, showing that July 2021 was generally warmer than July 2005. Such a significant increase reflects a notable shift in local climate conditions and a general temperature rise. The rise in temperature, particularly at night, suggests milder nighttime conditions and a reduced cooling effect, highlighting the impact of impervious surfaces and other factors on local climate dynamics.

The 2005 NDVI analysis of the Eryaman and its surroundings—the Eryaman, Alsancak, Ahi Mesut, and Elvankent neighborhoods of Etimesgut—shows that due to the presence of green spaces and barren land, the LST values were generally lower and more moderate. However, by 2021, an increase in LST was observed in these neighborhoods. This indicates that the rise in built-up areas contributed to higher LST, again highlighting the impact of large-scale residential areas on local thermal conditions.

The changes in vegetation, assessed by NDVI, influence LST. However, the rise in temperatures is not solely dependent on the amount of vegetation but is also associated with climate change and other environmental factors. This highlights the complex interplay between

urban development, vegetation loss, and broader climatic and environmental changes, pointing to increasing LST values.

The Difference in LST Between 2005 and 2021: The LST values show a difference of -2 to 6 degrees between 2005 and 2021 (Figure 6).

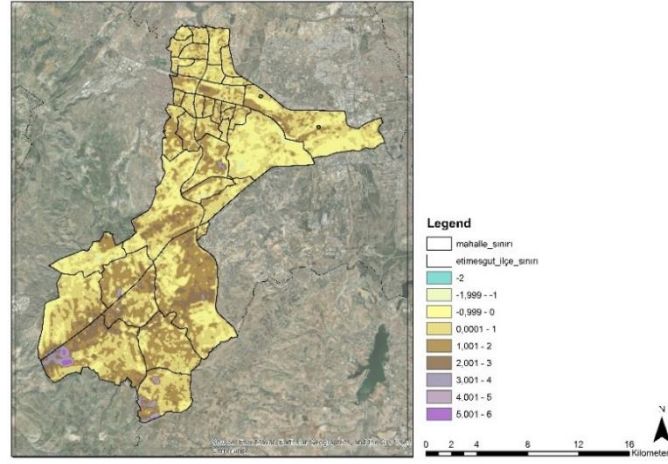


**Figure 6. Difference in LST for Etimesgut District between 2005 and 2021.**

When examining the LST differences, it is observed that temperatures have decreased in some areas and increased in others, indicating cooling in certain regions and warming in others. Areas where LST has dropped by up to  $-2^{\circ}\text{C}$  may have experienced cooling due to environmental or microclimatic factors. These factors could include increased vegetation (which provides cooling through evapotranspiration), changing wind patterns, higher rainfall, or human-induced changes. In the recently developed neighborhoods of Bağlıca, Yaprıcak, Etiler, Yeşilova, Ballıkuyumcu, and Yukarı Yurtçu, the surface temperature (LST) differences range between  $3^{\circ}\text{C}$  and  $6^{\circ}\text{C}$ .

The LST difference across Etimesgut between 2005 and 2021 shows a notable increase, particularly in the Bağlıca and Yaprıcak neighborhoods. Rapid urban development, the reduction of vegetation, and increased urban density in these areas have led to a rise in LST. In contrast, the Eryaman, Alsancak, Ahi Mesut, and Elvankent neighborhoods show a smaller temperature difference. This may indicate that green spaces have been better preserved in these areas than Bağlıca and Yaprıcak neighborhoods and that urban development has been more limited, with growth occurring in a more balanced way.

LULC: LULC data for July 2005 and 2021 was obtained using satellite images through maximum likelihood classification, one of the supervised classification methods. As shown in

Figure 7, the LULC was categorized as settlement areas, forest areas, vegetation, barren land, and water bodies.

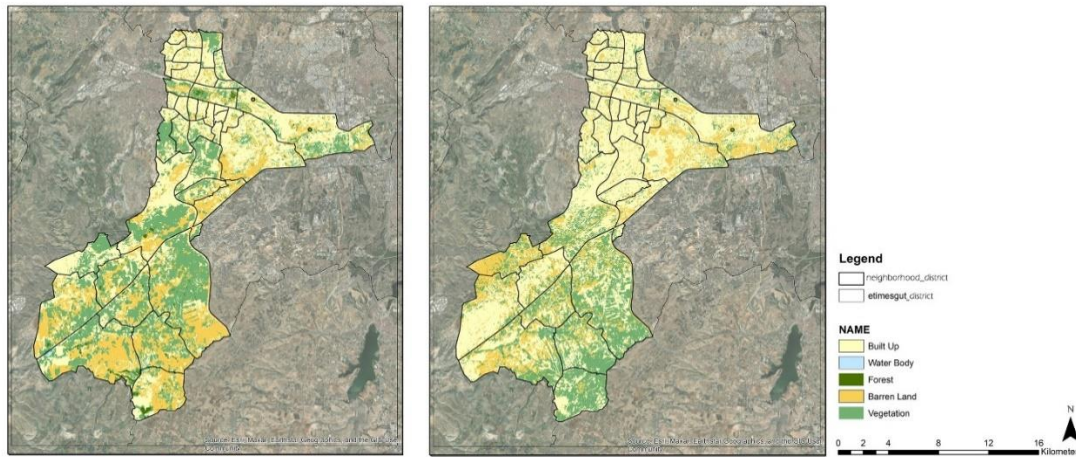


**Figure 7. (a) LULC of Etimesgut District (2005), (b) LULC of Etimesgut District (2021).**

As of 2005, the urbanized area in Etimesgut district covered approximately 9,040 hectares, while by 2021, this area had expanded to around 12,934 hectares, reflecting a 43.07% increase. In contrast, agricultural and forest land decreased from 7,697 hectares in 2005 to 5,347 hectares in 2021, marking a 30.53% decline. The land cover analysis indicates that from 2005 to 2021, forest and agricultural areas lost their characteristics, while built-up areas continued to expand partially.

The analysis shows that in 2005, the Eryaman, Alsancak, Ahi Mesut, and Elvankent neighborhoods had a high density of forests and vegetation, with relatively limited urban development. However, by 2021, these neighborhoods experienced fewer green spaces and more built-up areas. In contrast, also supported by the NDVI and LST analysis, the Bağlıca and Yaprıcık neighborhoods in 2005 had large areas of green and barren land with minimal development. By 2021, these areas underwent significant urban transformation, with urban areas expanding notably, particularly in Bağlıca and Yaprıcık, where green spaces were significantly reduced.

**Road Network Analysis:** The road network analysis reveals that the total road length increased from 1,107.56 km in 2005 to 1,773.08 km in 2021, representing an approximate increase of 60.08% (Figure 8 (a), (b)).



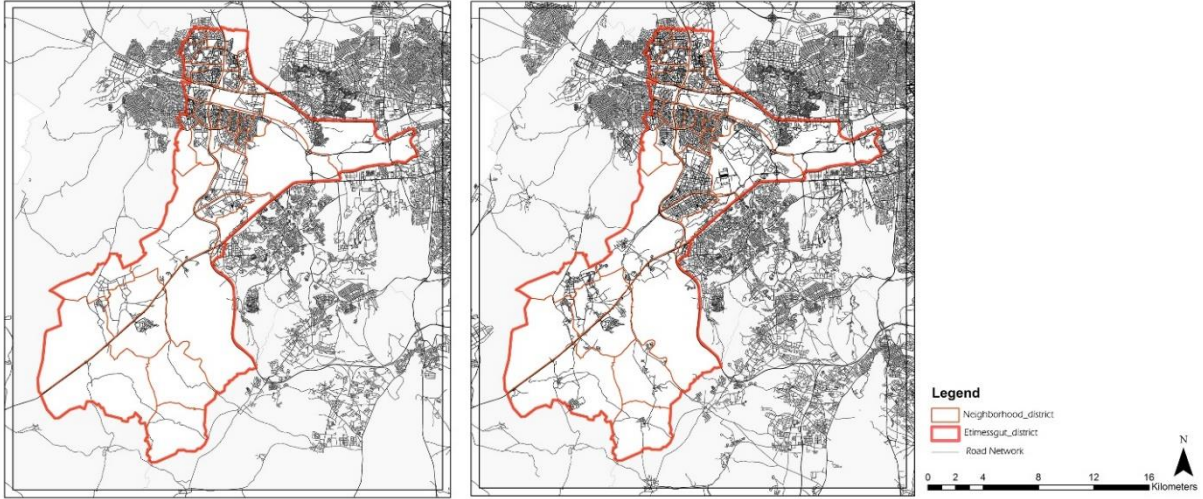


**Figure 8. (a) Road Network Analysis of Etimesgut District (2005), (b) Road Network Analysis of Etimesgut District (2021).**

The increase in road network length not only reflects economic growth and development but also serves as a significant indicator of urban expansion. An increasing population drives the need for more residential areas, business spaces, and services, leading to the expansion of cities and the construction of new roads. This process of urban growth, while addressing the demands of a growing population, contributes to rising surface temperatures due to the replacement of vegetated areas with impervious surfaces [39].

The analysis shows that in 2005, for example, the Eryaman, Alsancak, Ahi Mesut and Elvankent neighborhoods had a well-developed road network and established urban infrastructure, which is why there was little expansion in these areas by 2021. However, in the Bağlıca and Yaprıcık neighborhoods, the road network in 2005 was quite limited, with these areas predominantly rural and covered with green spaces. By 2021, the road network expanded significantly with the acceleration of large-scale residential development in the Bağlıca and Yaprıcık neighborhoods.

**Building Footprint Analysis:** When examining the changes between 2005 and 2021, the building footprint was calculated to be 6,625,205 m<sup>2</sup> in 2005 and 8,140,717 m<sup>2</sup> in 2021. The size of the building footprint increased by approximately 22.87% between 2005 and 2021 (Figure 9 (a), (b)).

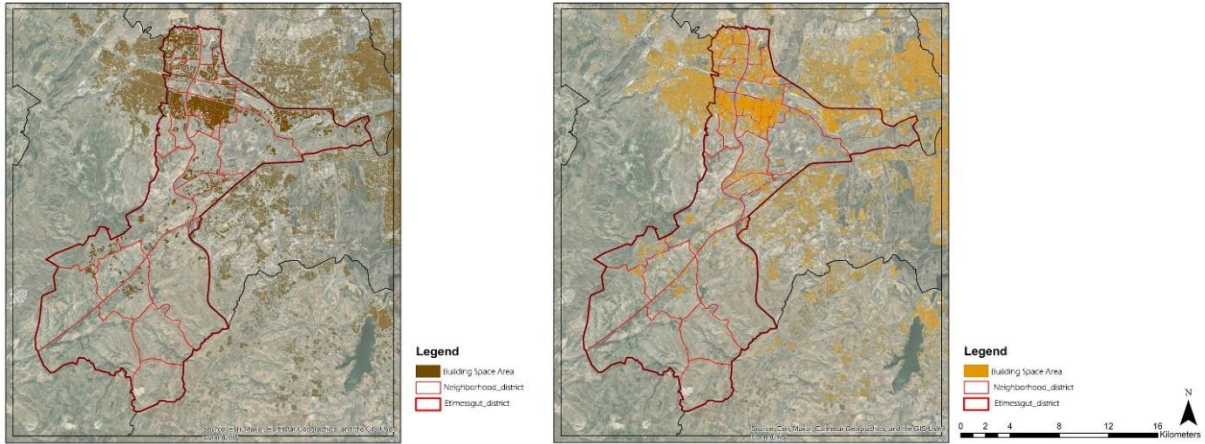


**Figure 9. (a) Building Footprint Analysis of Etimesgut District (2005), (b) Building Footprint Analysis of Etimesgut District (2021).**

This increase in the building footprint in the Etimesgut district is a clear indicator of urban development, which signifies the district's expansion with new large-scale residential areas and the intensification of the built-up areas, driven by population growth.

Denser built-up areas and the development of new housing projects typically progress in parallel with population growth, economic development, and infrastructure investments. In the case of Etimesgut, from 2005 to 2021, there was both physical expansion and an increase in building density. Between 2005 and 2021, significant urban development occurred across the district, with a notable increase in building footprint, particularly in the Bağlıca and Yaprıcık neighborhoods. In Bağlıca, the total building footprint area increased from 277,452 m<sup>2</sup> in 2005 to 439,468 m<sup>2</sup> in 2021, reflecting a growth of 58.39%. This expansion was accompanied by an increase in neighborhood density, which rose from 0.06 in 2005 to 0.1 in 2021, indicating a significant intensification of the built environment. In Yaprıcık, the total building footprint area grew from 213,832 m<sup>2</sup> to 218,161 m<sup>2</sup> during the same period, indicating a 2.02% increase.

In the Eryaman, Alsancak, Ahi Mesut, and Elvankent neighborhoods, where built-up areas are already high, there was a partial increase in density. In Elvankent neighborhood, the total building footprint increased from 226,285 m<sup>2</sup> in 2005 to 235,749 m<sup>2</sup> in 2021, reflecting a growth of 4.18%, in Alsancak neighborhood, increased from 137,884 m<sup>2</sup> to 201,753 m<sup>2</sup>, showing a 46.31%, in Eryaman neighborhood, increased from 150,598 m<sup>2</sup> to 233,793 m<sup>2</sup>, marking a 55.25% rise, and in Ahi Mesut neighborhood, increased from 93,433 m<sup>2</sup> to 209,135 m<sup>2</sup>, achieving a notable increase of 123.81%. In Elvankent, this value rose from 0,17 m<sup>2</sup> to 0,18 m<sup>2</sup>, in Alsancak from 0,12 m<sup>2</sup> to 0,18 m<sup>2</sup>, in Eryaman from 0,06 m<sup>2</sup> to 0,1 m<sup>2</sup>, and in Ahi Mesut

from 0,03 m<sup>2</sup> to 0,08 m<sup>2</sup>. These changes indicate that larger-scale residential development is more intense in the Bağlıca and Yapracık neighborhoods of Etimesgut.

Perceived Air Temperature Spatial Interpolation Analysis (IDW): Spatial Interpolation Analysis is a function that represents the entire surface and predicts values at other points or sub-areas based on a set of discrete points or sub-areas given as spatial data [30]. Inverse distance weighing (IDW) performs a surface interpolation based on the weighted average of sample points, reducing the weight as the distance from the interpolated point increases [31]. The interpolation of average minimum and maximum temperatures across the district was calculated using the daily average minimum and maximum temperature values from the station data for 2005 and 2021 (Figures 10-11).

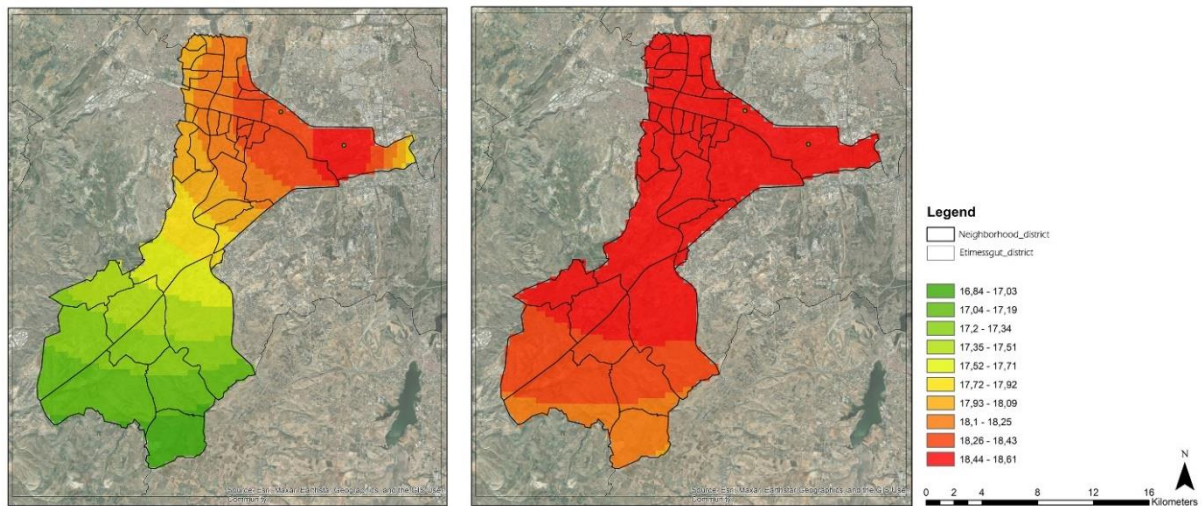


**Figure 10. (a) Building Footprint Analysis of Etimesgut District (2005), (b) Building Footprint Analysis of Etimesgut District (2021).**

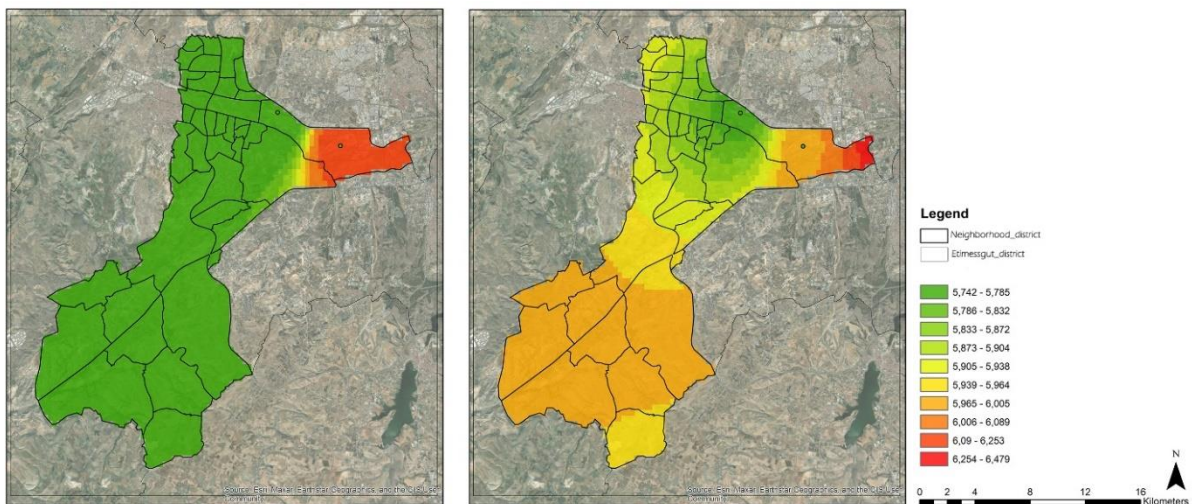


**Figure 11. (a) Building Footprint Analysis of Etimesgut District (2005), (b) Building Footprint Analysis of Etimesgut District (2021).**

In the temperature maps obtained through interpolation calculations, the average minimum and maximum temperature values show that in 2005, the average minimum temperature ranged between 5.52°C and 6.20°C (Figure 10 (a)), while the average maximum temperature ranged between 16.84°C and 18.61°C (Figure 11 (a)). In 2021, the average minimum temperature ranged between 5.74°C and 6.47°C (Figure 10 (b)), while the average maximum temperature ranged between 18.08°C and 19.30°C (Figure 11 (b)).

In Figure 12, the average hourly relative humidity (%) was calculated based on data from the Etimesgut Airport and Ankara Güvercinlik Airport stations in the Etimesgut district for 2005 and 2021. Accordingly, in 2005, the average hourly relative humidity at Etimesgut Airport was measured at 68.84%, while in 2021, this rate decreased to 61.19%. This indicates a decrease of approximately 7.65% in relative humidity between 2005 and 2021. For Ankara Güvercinlik Airport, data is not available for 2005, but it is recorded at 58.40% for 2021. We cannot assess the difference due to a lack of data at Ankara Güvercinlik Airport.

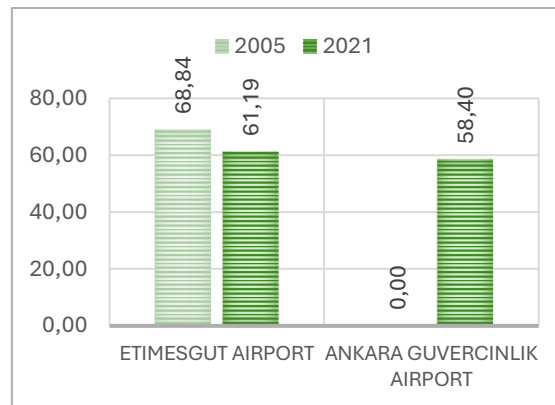


**Figure 12. Average Hourly Relative Humidity (%).**

In Figure 13, we compared the total precipitation in kilograms per square meter ( $\text{mm} = \text{kg/m}^2$ ) for 2005 and 2021, based on data from the Etimesgut Airport and Ankara Güvercinlik Airport stations. At Etimesgut Airport, the precipitation per square meter in 2005 was 1.10 kg; in 2021, this amount decreased by 5.45% to 1.04 kg. At Ankara Güvercinlik Airport, the precipitation in 2005 was measured at 1.08 kg, but by 2021, it had decreased by 21.30% to 0.85 kg. A reduction in precipitation is observed at both airports in 2021 compared to 2005; however, the decrease at Ankara Güvercinlik Airport is more significant than at Etimesgut Airport. This difference may be related to precipitation volume, as well as influenced by microclimatic effects, surface changes, urbanization differences, and airflows [42].

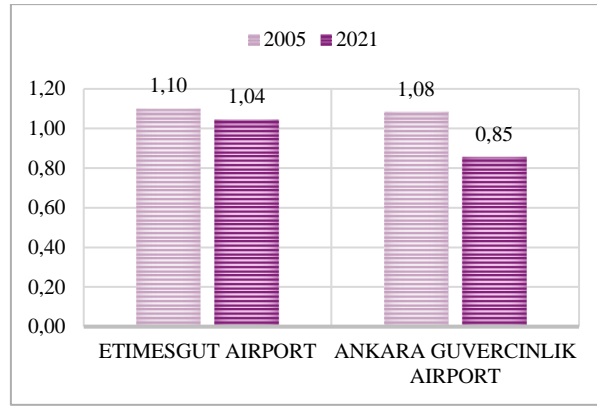


**Figure 13. Total Precipitation ( $\text{mm} = \text{kg}/\text{m}^2$ ) – Kilograms of Precipitation per Square Meter.**

Figure 14 presents the average wind speeds for 2005 and 2021 based on data from the Etimesgut Airport and Ankara Güvercinlik Airport stations. At Etimesgut Airport, the average wind speed was recorded at 1.45 m/s in 2005, which increased by 72.41% to 2.50 m/s in 2021. At Ankara Güvercinlik Airport, the average wind speed in 2005 was 0.34 m/s, and it rose dramatically by 552.94% to 2.22 m/s in 2021. Both airports experienced a significant increase in average wind speeds, with the rise at Ankara Güvercinlik Airport being much more significant.

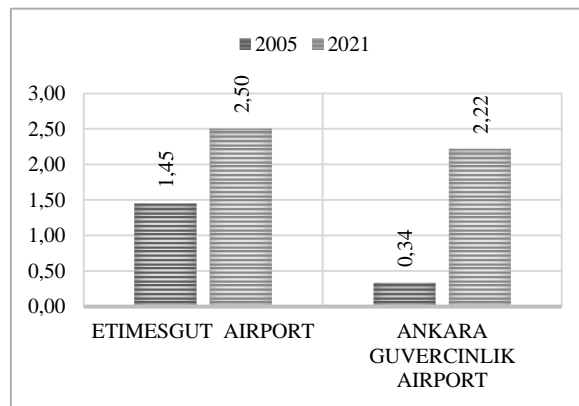


**Figure 14. Average Wind Speed (m/s- meters per second).**

In urban areas, relative humidity (%), precipitation, and wind speed influence changes in the average minimum and maximum temperature values. A wind speed interpolation was conducted across the central district using the average wind speed values from the measurement station data for 2005 and 2021. The results indicate that the change in wind speed shows similarities to the temperature interpolation results, with the observation that as wind speed increases, the measured temperature in the city decreases.

Population Projection Calculation: Figure 15 shows the population change in Etimesgut district for 2005 and 2021. The population of Etimesgut was 272,977 in 2005, and in 2021, it rose to 606,472, a 122% increase from 2005 to 2021. This indicates that the district has experienced significant population growth, which suggests that the development of new large-scale residential areas in Etimesgut has significantly influenced this growth process.

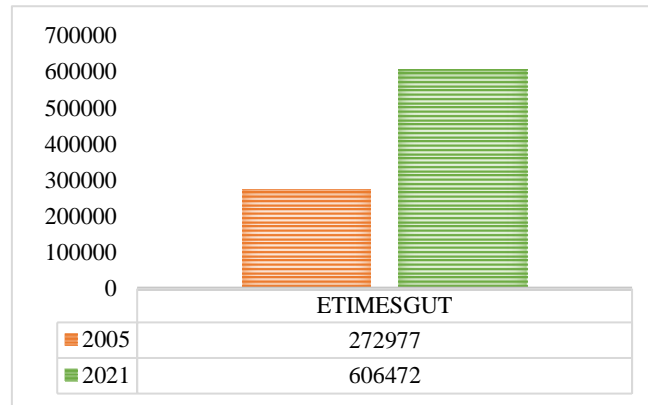


Figure 15. Total Population Change in Etimesgut District.

Profile Analysis: Analyzing the temperature variations along a profile line shows the LST profile change between points A and B in the Etimesgut district for 2005 and 2021 (Figure 16).

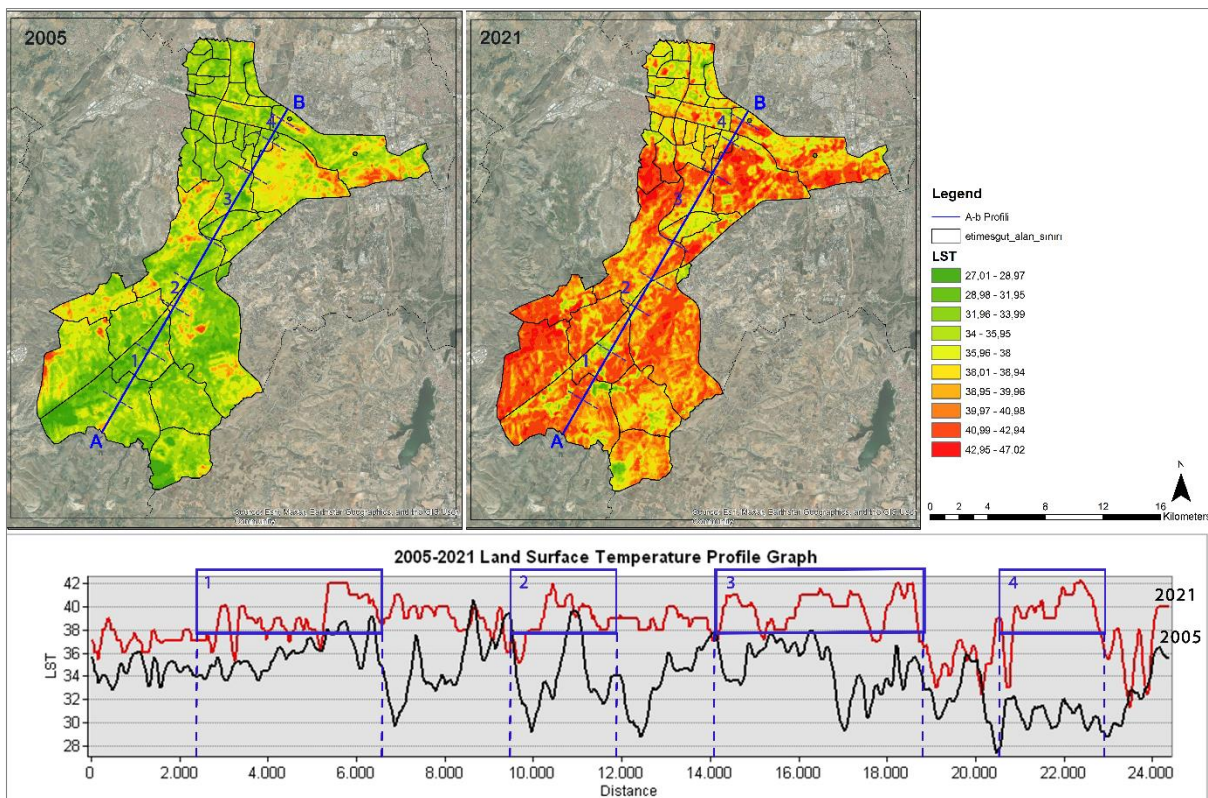


Figure 16. LST Profile Analysis of Etimesgut District (2005-2021).

On the map, green colors represent lower temperatures (27.01-28.97°C), while red and orange indicate higher temperatures (42.95-47.02°C). The temperatures from point A to point B in 2021 are generally higher compared to 2005. For example, within the 0-10 km range, temperatures ranged between 28-34°C in 2005, whereas in 2021, these values increased to a range between 36-40°C.

The UHI effect causes an increase in LST in areas with dense built-up increases. This effect results from buildings, asphalt roads, and other construction materials absorbing sunlight, releasing it slowly, and restricting airflow. The Etimesgut district has undergone an urbanization process since the 1990s, which accelerated in the 2000s. In particular, the neighborhoods of Eryaman, Elvankent, and Ahi Mesut began to develop in the 1990s, but rapid urbanization took place in the 2000s. In contrast, Bağlıca and Yapracık experienced a rapid construction boom after 2005. These neighborhoods previously exhibited more rural characteristics; however, after 2005, they gained an urban identity with increased housing projects. Between 2005 and 2021, a significant rise in LST was observed in the Etimesgut district. In 2005, particularly in the Bağlıca, Yapracık and Şehit Osman Avcı neighborhoods and the Eryaman, Alsancak, Ahi Mesut and Elvankent neighborhoods, lower LST and large green spaces were notable. However, by 2021, with the increase in built-up areas, LST in these neighborhoods rose to as high as 43°C. The UHI effect has intensified, especially in the Bağlıca and Yapracık neighborhoods, where urban spaces have replaced green spaces.

The profile graph illustrates the differences in temperature changes between points A and B. Significant spatial and temporal variations are observed. In Region 1, which consists of agricultural areas, surface temperatures were relatively lower in 2005; however, a noticeable increase is evident in 2021. This change can be attributed to the impact of agricultural activities, such as planting, harvesting, and soil processing, on surface temperature. Conversely, Regions 2, 3, and 4 exhibited lower temperatures in 2005 but experienced a significant increase in 2021. Increased urbanization, reduced surface permeability, and the intensification of the urban heat island (UHI) effect can explain this temperature rise.

#### **4 CONCLUSION AND SUGGESTIONS**

Since the 1950s, the city center, shaped by geomorphological thresholds, has concentrated in a basin, developing settlement areas with rapid population growth and new urban expansions. In recent years, debates on climate change and a general rise in temperatures have intensified. Research-based analyses have highlighted these effects, providing guidance

for urban policy and decision-making. This study demonstrates the increased spatiotemporal factors associated with the urban heat island (UHI) effect caused by built-up areas, particularly large-scale residential developments.

With the decentralization policies introduced by the 1990 Master Plan, the city's growth has expanded onto productive agricultural and public lands, primarily in the western region. With an economic emphasis on the construction sector, the residential development process has resulted in urban sprawl and population growth, particularly in the last three decades. This study examines the climate change impacts of this strategy through an analysis of the Etimesgut district in western Ankara. While the district includes other land use types, large-scale residential areas dominate.

Etimesgut, initially characterized by agricultural and public land, has experienced rapid urban development since the 1980s, with mass housing and large-scale residential developments by the Housing Development Agency. After the 1990s, rapid urbanization significantly transformed the district's built environment and natural surroundings. During this period, local and central administrations' planning policies promoted the creation of modern residential areas. However, this process often resulted in a fragmented and unsustainable urban fabric, particularly in areas with intensive housing development. Over time, Etimesgut, seen as a zone of mixed-use and transition, has evolved into an important satellite city of Ankara.

One significant impact of the development processes in Etimesgut is the prevalence of built-up areas with impervious surfaces, reduced barren land, and increased heat. Large asphalt roads, concrete multistorey structures, and other non-permeable surfaces built on agricultural land disrupt the natural water cycle by accumulating heat and surface water, leading to microclimate changes and intensifying the urban heat island (UHI) effect. Analysis of NDVI, LST, LULC, road networks, building footprints, and population changes reveals the extent of these impacts. Changes in climatic factors, such as relative humidity, total precipitation, and average wind speed, further support these findings. Profile analysis also highlights the overall LST changes across the district, providing strong evidence of the evolving UHI characteristics due to spatial development and zoning strategies, especially with converting agricultural land into large-scale residential areas.

Between 2005 and 2021, urban development and construction processes in Etimesgut significantly affected vegetation and surface temperatures, as evidenced by NDVI and LST data. The pronounced UHI effect in neighborhoods such as Bağlıca, Yapraklı and Eryaman



underscores the critical need for preserving and expanding green spaces in urban planning. Although some neighborhoods saw improvements in plant cover by 2021, urbanization and global warming have led to significant surface temperature increases, highlighting these developments' environmental and climatic challenges.

This situation emphasizes the necessity of sustainable urban planning in Etimesgut. Preserving green and agricultural areas, carefully managing urban growth, and mitigating the UHI effect through sustainable strategies are vital for reducing environmental and climatic impacts.

The literature presents several studies at multiple scales; some focus on the UHI effect of recently built developments in a city [10], [11], while others, with a broader approach, analyze regions within a country [15], [34]. This study, conducted at the district level, highlights changes in selected neighborhoods where land use has recently shifted from agriculture to large-scale residential areas. This study is useful for identifying changes in UHI assessment factors and aims to inform urban policy-making by providing a pathway from research to actionable strategies. By exploring UHI assessment factors, we identified specific strategies and visualized them on maps to assist policymakers. Conducting similar analyses at smaller scales could further guide neighborhood development and regeneration policies, shaping urban design and planning.

The relationship between NDVI and LST reveals that changes in plant cover significantly influence surface temperatures. However, the rise in temperatures is not solely due to vegetation loss; climate change and other environmental factors also contribute. Despite some improvements in plant cover in 2021, surface temperature increases caused by global warming and local development remain evident. This highlights cities' need to align their plans with broader climate policies. In Etimesgut, a significant rise in surface temperatures was observed between 2005 and 2021, particularly in neighborhoods such as Bağlıca, Yaprıcık, and Eryaman, where intensive construction activity has occurred. This increase reflects the intensification of the UHI effect across the region.

The reduction of green spaces and intensive urban development have disrupted the environmental balance and elevated surface temperatures. Sustainable urban planning is critical in mitigating these impacts by increasing green spaces and addressing climate change. The preservation of natural areas is essential for the sustainable development of Etimesgut, requiring careful planning to integrate new green spaces and minimize the environmental impacts of

urbanization. Adopting sustainable urbanization principles is mandatory to combat climate change and promote eco-friendly urban growth. Balanced urbanization will improve the quality of life for residents while supporting environmental sustainability.

Studies on the urban heat island effect in Ankara address topics such as the impact of land use and cover changes caused by the increase in built-up areas on surface temperatures, the social, economic, environmental, institutional, and spatial dimensions of vulnerability to climate change, and the contributions of urban transformation practices to this effect [35], [36], [37]. As a unique example from Ankara, Turkey, this analysis in the Etimesgut district implies that both local and central governments should develop urban policies, programs, and strategies to mitigate the UHI effect as climate change has become more evident in recent years. For example, developing new zoning for integrating green spaces and less impervious surfaces into large-scale residential area developments and enforcing such regulations as development moratoriums of the construction companies can benefit both the inhabitants of the residential area and the city dwellers. In addition, adopting energy-friendly construction materials and limiting the height of the new developments in certain areas can be some of the policies that can be enhanced.

There is a growing concern in Turkey about developing a holistic urban planning and design framework for new residential developments. The aim is to integrate these developments into a compact urban form that fosters connections and promotes sustainability. The thermal governance approach focuses on engaging people in the public realm, enabling them to live, work, and socialize, thereby enhancing community ties. At the same time, this approach helps mitigate the UHI effect by promoting green infrastructure and facilitating sustainable commuting options, such as cycling and walking. Decision-makers should prioritize balancing built-up areas with green spaces and include natural cooling mechanisms in their plans. Such urban planning policies will improve the urban environment and reduce the climatic impacts of UHI formation, ultimately benefiting the community.

Land cover analysis reveals significant changes, including the loss of agricultural and forest lands and increased impervious surfaces. The reduction of green spaces and the dominance of non-permeable surfaces have contributed to rising surface temperatures, underscoring the urgent need to apply sustainability principles in city planning. To combat climate change, Etimesgut must invest in green infrastructure, including landscaped areas, wind corridors, and parks. These measures should also include increasing tree cover, implementing green and cool roofs, and integrating such features into buildings and public spaces. Combining

these initiatives with urban planning focused on environmental sustainability will mitigate urban thermal issues and support the realization of sustainable green policies.

### **Acknowledgment**

This study is derived from the doctoral thesis "Fractal Analysis of the Impact of Urban Growth on Urban Heat Island Formation."

### **Conflict of Interest Statement**

There is no conflict of interest between the authors.

### **Statement of Research and Publication Ethics**

The study is complied with research and publication ethics

### **Artificial Intelligence (AI) Contribution Statement**

This manuscript was entirely written, edited, analyzed, and prepared without the assistance of any artificial intelligence (AI) tools. All content, including text, data analysis, and figures, was solely generated by the authors.

### **Contributions of the Authors**

All authors contributed equally.

### **REFERENCES**

- [1] C. Altenburg, "Chapter 1 institutional and social capacities in lead cities in Europe and the United States: Success factors for urban sustainability?," in *Research in Urban Sociology*, Emerald Group Publishing Limited, 2012, pp. 3–28.
- [2] J.-H. Chang, "Thermal governance, urban metabolism and carbonised comfort: Air-conditioning and urbanisation in the Gulf and Doha," *Urban Stud.*, vol. 61, no. 15, pp. 2928–2944, 2024.
- [3] F. Musco, Ed., *Counteracting urban heat island effects in a global climate change scenario*. Cham: Springer International Publishing, 2016.
- [4] V. Costanzo, G. Evola, and L. Marletta, *Urban heat stress and mitigation solutions: An engineering perspective*. London, England: Taylor & Francis, 2021.
- [5] N. Badaro-Saliba, J. Adjizian-Gerard, R. Zaarour, and G. Najjar, "LCZ scheme for assessing Urban Heat Island intensity in a complex urban area (Beirut, Lebanon)," *Urban Clim.*, vol. 37, no. 100846, p. 100846, 2021.

- [6] P. Singh, N. Kikon, and P. Verma, "Impact of land use change and urbanization on urban heat island in Lucknow city, Central India. A remote sensing based estimate," *Sustain. Cities Soc.*, vol. 32, pp. 100–114, 2017.
- [7] U. Rajasekar and Q. Weng, "Urban heat island monitoring and analysis using a non-parametric model: A case study of Indianapolis," *ISPRS J. Photogramm. Remote Sens.*, vol. 64, no. 1, pp. 86–96, 2009.
- [8] R. Paolini and M. Santamouris, *Urban Climate Change and Heat Islands: Characterization, impacts, and mitigation*. Elsevier, 2022.
- [9] A. Ali and Z. Alam Nayyar, "A Modified Built-up Index (MBI) for automatic urban area extraction from Landsat 8 Imagery," *Infrared Phys. Technol.*, vol. 116, no. 103769, p. 103769, 2021.
- [10] R. Neog, "Analyzing dynamic behavior of land use and land surface temperature in the city of Imphal, India," *Acta Geophys.*, vol. 69, no. 6, pp. 2275–2290, 2021.
- [11] X. Zhou and H. Chen, "Impact of urbanization-related land use land cover changes and urban morphology changes on the urban heat island phenomenon," *Sci. Total Environ.*, vol. 635, pp. 1467–1476, 2018.
- [12] P. Mohammad, A. Goswami, S. Chauhan, and S. Nayak, "Machine learning algorithm based prediction of land use land cover and land surface temperature changes to characterize the surface urban heat island phenomena over Ahmedabad city, India," *Urban Clim.*, vol. 42, no. 101116, p. 101116, 2022.
- [13] O. A. Fashae, E. G. Adagbasa, A. O. Olusola, and R. O. Obateru, "Land use/land cover change and land surface temperature of Ibadan and environs, Nigeria," *Environ. Monit. Assess.*, vol. 192, no. 2, 2020.
- [14] A. Achmad, N. Fadhly, A. Deli, and I. Ramli, "Urban growth and its impact on land surface temperature in an industrial city in Aceh, Indonesia," *Lett. Spat. Resour. Sci.*, vol. 15, no. 1, pp. 39–58, 2022.
- [15] N. I. Molina-Gómez, L. M. Varon-Bravo, R. Sierra-Parada, and P. A. López-Jiménez, "Urban growth and heat islands: A case study in micro-territories for urban sustainability," *Urban Ecosyst.*, vol. 25, no. 5, pp. 1379–1397, 2022.
- [16] M. Carpio, Á. González, M. González, and K. Verichev, "Influence of pavements on the urban heat island phenomenon: A scientific evolution analysis," *Energy Build.*, vol. 226, no. 110379, p. 110379, 2020.
- [17] K. J. Gohain, P. Mohammad, and A. Goswami, "Assessing the impact of land use land cover changes on land surface temperature over Pune city, India," *Quat. Int.*, vol. 575–576, pp. 259–269, 2021.
- [18] A.-. A. Kafy, A.-A.- Faisal, A. Al Rakib, M. A. Fattah, Z. A. Rahaman, and G. S. Sattar, "Impact of vegetation cover loss on surface temperature and carbon emission in a fastest-growing city, Cumilla, Bangladesh," *Build. Environ.*, vol. 208, no. 108573, p. 108573, 2022.
- [19] R. J. Corner, A. M. Dewan, and S. Chakma, "Monitoring and prediction of land-use and land-cover (LULC) change," in *Dhaka Megacity*, Dordrecht: Springer Netherlands, 2014, pp. 75–97.
- [20] M. Waleed and M. Sajjad, "Warming cities in Pakistan: Evaluating spatial-temporal dynamics of urban thermal field variance index under rapid urbanization," in *Urban Sustainability*, Singapore: Springer Nature Singapore, 2023, pp. 67–82.
- [21] B. Ahmed, M. Kamruzzaman, X. Zhu, M. Rahman, and K. Choi, "Simulating land cover changes and their impacts on land surface temperature in Dhaka, Bangladesh," *Remote Sens. (Basel)*, vol. 5, no. 11, pp. 5969–5998, 2013.
- [22] "Nüfus İstatistikleri Portalı," Gov.tr. [Online]. Available: <https://nip.tuik.gov.tr/>. [Accessed: 04-Dec-2024].
- [23] "2023 Başkent Ankara Nazım İmar Planı," Bel.tr. [Online]. Available: <https://www.ankara.bel.tr/ankara-buyuksehir-belediyesi-nazim-plan>. [Accessed: 04-Dec-2024].
- [24] B. Günay, "Ankara çekirdek alanının oluşumu ve 1990 nazım planı hakkında bir değerlendirme," in *Cumhuriyet'in Ankara'sı*, T. Şenyapılı, Ed. Ankara, Türkiye: ODTÜ Geliştirme Vakfı Yayıncılık, 2005, pp. 60–118.
- [25] *Usgs.gov*. [Online]. Available: <https://www.usgs.gov/landsat-missions/landsat-8-data-users-handbook>. [Accessed: 04-Dec-2024].

- [26] N. Nazarian and L. Norford, "Measuring and assessing thermal exposure," in *Urban Heat Stress and Mitigation Solutions*, London: Routledge, 2021, pp. 40–61.
- [27] Y. Ghobadi, B. Pradhan, H. Z. M. Shafri, and K. Kabiri, "Assessment of spatial relationship between land surface temperature and landuse/cover retrieval from multi-temporal remote sensing data in South Karkheh Sub-basin, Iran," *Arab. J. Geosci.*, vol. 8, no. 1, pp. 525–537, 2015.
- [28] Q. Weng, D. Lu, and J. Schubring, "Estimation of land surface temperature–vegetation abundance relationship for urban heat island studies," *Remote Sens. Environ.*, vol. 89, no. 4, pp. 467–483, 2004.
- [29] *Academia.edu*. [Online]. Available: <https://www.academia.edu/download/56616293/IJET-V4I1P4.pdf>. [Accessed: 04-Dec-2024].
- [30] N. S.-N. Lam, "Spatial interpolation methods: A review," *Am. Cartogr.*, vol. 10, no. 2, pp. 129–150, 1983.
- [31] A. İlker, Ö. Terzi, and E. Şener, "Yağışın Alansal Dağılımının Haritalandırılmasında Enterpolasyon Yöntemlerinin Karşılaştırılması: Akdeniz Bölgesi Örneği," *Tek. Dergi*, vol. 30, no. 3, pp. 9213–9219, 2019.
- [32] K. M. Çubukçu, *Planlamada Klasik Sayısal Yöntemler*. Ankara, Türkiye: ODTÜ Geliştirme Vakfı, 2008.
- [33] M. E. Hereher, "Assessment of seasonal warming trends at the Nile Delta: a paradigm for human-induced climate change," *Environ. Monit. Assess.*, vol. 196, no. 1, 2024.
- [34] *Researchgate.net*. [Online]. Available: [https://www.researchgate.net/publication/346534911\\_Effects\\_of\\_urban\\_growth\\_on\\_the\\_land\\_surface\\_temperature\\_a\\_case\\_study\\_in\\_Taiyuan\\_China](https://www.researchgate.net/publication/346534911_Effects_of_urban_growth_on_the_land_surface_temperature_a_case_study_in_Taiyuan_China). [Accessed: 04-Dec-2024].
- [35] *Org.tr*. [Online]. Available: <https://dergipark.org.tr/en/pub/gazimmfd/issue/6678/88558>. [Accessed: 04-Dec-2024].
- [36] *Org.tr*. [Online]. Available: <https://dergipark.org.tr/en/pub/sdufenbed/article/221982>. [Accessed: 04-Dec-2024].
- [37] *Edu.tr*. [Online]. Available: <https://open.metu.edu.tr/handle/11511/58936>. [Accessed: 04-Dec-2024].
- [38] H. Yıldız, A. Mermer, E. Ünal, ve F. Akbaş, "Türkiye Bitki Örtüsünün NDVI Verileri ile Zamansal ve Mekansal Analizi", *Tarla Bitkileri Merkez Araştırma Enstitüsü Dergisi*, c. 21, sy. 2, ss. 50–56, 2012.
- [39] I. D. Stewart and G. Mills, *The Urban Heat Island*. Elsevier, 2021.
- [40] M. N. Rahman, M. R. H. Rony, F. A. Jannat, S. C. Pal, M. S. Islam, E. Alam, and A. R. M. T. Islam, "Impact of Urbanization on Urban Heat Island Intensity in Major Districts of Bangladesh Using Remote Sensing and Geo-Spatial Tools," *Climate*, vol.10, no.1, p.3, 2022.
- [41] T. Şenyapılı, *Baraka'dan Gecekonduya*. İstanbul: İletişim Yayınları, 2004.
- [42] L. Hao, G. Sun, X. Huang, R. Tang, K. Jin, Y. Lai, D. Chen, Y. Zhang, D. Zhou, Z.-L. Yang, L. Wang, G. Dong, and W. Li, "Urbanization alters atmospheric dryness through land evapotranspiration," *npj Climate and Atmospheric Science*, vol. 6, Art. no. 149, Sep. 2023. [Online]. Available: <https://doi.org/10.1038/s41612-023-00429-x>.